



**MODELLING OF A FIXED BED ADSORBER BASED ON AN ISOTHERM MODEL
OR AN APPARENT KINETIC MODEL**

**MODELADO DE UN ADSORBEDOR DE LECHO FIJO BASADO EN UN MODELO
DE ISOTERMA O UN MODELO CINÉTICO APARENTE**

G. Che-Galicia, C. Martínez-Vera, R.S. Ruiz-Martínez* and C.O. Castillo-Araiza*

Grupo de Procesos de Transporte y Reacción en Sistemas Multifásicos, Depto. de IPH, Universidad Autónoma Metropolitana - Iztapalapa, Av. San Rafael Atlixco No. 186, C.P. 09340, México D.F., Mexico.

Received March 5, 2014; Accepted May 20, 2014

Abstract

Isotherm model and apparent kinetic model are simple approaches, which are indistinctly used to predict the kinetic behaviour of the adsorption phenomena. The main objective in this work was to elucidate when these approaches should be coupled to a pseudo-heterogeneous fixed-bed adsorber model to describe reliable breakthrough curves when experimental data at industrial scale are not available. To achieve this, an adsorption column packed with a low-cost natural zeolite was modelled for the removal of Rhodamine B (RhB). To have certainty in the model predictions, equilibrium and kinetic experiments were carried out. Freundlich isotherm model and a pseudo second order apparent kinetic model accounting for diffusion phenomena led to the most adequate fit to experimental data. Experimental and simulations results indicated that the use of an isotherm model (LDF-M) or an apparent kinetic model (AkA-M) in the packed bed adsorbed model predicted similar tendencies regarding the effect on the breakthrough point of the different parameters considered. Nevertheless, the shapes of the breakthrough curves predicted by both models were significantly different, suggesting that an apparent kinetic model is necessary to have reliable prediction of the industrial behaviour of this studied zeolite since intraparticle mass transport resistances are significant.

Keywords: packed bed adsorber, breakthrough curves, adsorption kinetics, isotherm model, apparent kinetic model.

Resumen

Los modelos de isotermas y de cinética aparentes de adsorción son aproximaciones indistintamente utilizadas para describir el comportamiento de un determinado adsorbato-adsorbente. El objetivo principal de este trabajo fue elucidar cuando estas aproximaciones deben ser acopladas a un modelo pseudo-heterogéneo de un adsorbedor de lecho fijo para describir curvas de ruptura confiables cuando no existen datos experimentales a escala industrial. Para lograr esto, se modeló una columna de adsorción empacada con una zeolita natural de bajo costo que no ha sido estudiada previamente para la remoción de Rodamina B (RhB). Para tener certidumbre en las predicciones del modelo, se llevaron a cabo experimentos de equilibrio y cinéticos. El modelo de la isoterma de Freundlich y un modelo cinético aparente de pseudo segundo orden que considera los fenómenos de difusión presentaron el mejor ajuste a los datos experimentales. Los resultados experimentales y las simulaciones indicaron que el modelado de un adsorbedor de lecho empacado con un modelo de isoterma (LDF-M) o un modelo cinético aparente (AkA-M), predice tendencias similares en relación con el efecto en el punto de ruptura de los diferentes parámetros considerados. Sin embargo, las formas de las curvas de ruptura predichas por ambos modelos fueron significativamente diferentes, lo que sugiere la necesidad de un modelo cinético aparente para describir el comportamiento industrial de esta zeolita debido a que las resistencias al transporte de masa por difusión en el adsorbente son significativas.

Palabras clave: adsorbedor de lecho empacado, curvas de ruptura, cinética de adsorción, modelo de isoterma, modelo cinético aparente.

*Corresponding author. E-mail: rmr@xanum.uam (R.S.R.M.); coca@xanum.uam.mx (C.O.C.A.)

1 Introduction

The removal of dyes from textile industry effluents is a critical problem worldwide, since these molecules are among the most common organic contaminants in groundwater wells and surface waters, causing adverse effects to organisms even at low concentrations due to their toxic properties (Hutzler *et al.*, 1986; Özcan *et al.*, 2005; Crini, 2006). There is hence the necessity to minimise the environmental release of dyes. A review of the advantages and disadvantages of conventional methods for the removal of harmful pollutants is discussed elsewhere (Robinson *et al.*, 2001). Adsorption is one of the most used and effective processes for the removal of synthetic dyes that are difficult to mineralise by conventional methods. Activated carbons have demonstrated their effectiveness in adsorbing this type of pollutant (Namasivayam and Kavitha, 2002). However, the high-cost of activated carbon and the costs associated with the adsorbent regeneration process have made these materials non-economically feasible for industrial use (Osma *et al.*, 2007). In this context, various low-cost adsorbents derived from agricultural waste, biosorbents, industrial waste-materials or natural materials have been investigated to eliminate synthetic dyes from industrial textile effluents (Rafatullah *et al.*, 2010). In particular, natural zeolites have gained commercial and environmental interest because of their worldwide abundance, low-cost, and profitable regeneration (Wang and Peng, 2010).

The design of industrial adsorbers requires some parameters that must be obtained from extensive laboratory and pilot plant experiments that are time consuming and expensive (Sankararao and Gupta, 2007). In this sense, modelling and simulation normally complement this aim, serving as major engineering tools to design and optimise the dynamic behaviour of fixed-bed adsorbers (Liao and Shiau, 2000; Inglezakis and Grigoropoulou, 2004). In the models used to predict breakthrough curves, mass transport phenomena are well understood and adequately described in the literature (Hall *et al.*, 1966; Wilson *et al.*, 1966; Ruthven, 1984). However, presently there is no unique modelling approach accepted to describe adsorption kinetics (Marshall and Pigford, 1947; Crittenden and Weber, 1978; Ko *et al.*, 2001; Ruthven, 1984; Tien, 1994; Romero-González *et al.*, 2005). In some of the approaches, it is assumed that the mobile and stationary phases instantly reach equilibrium, and hence make use of an

isotherm equilibrium model to account for adsorption kinetics (Hutzler *et al.*, 1986; Chern and Chien, 2001). Another approaches account for the surface dynamics between the mobile and stationary phases making use of a proper kinetic model or apparent kinetic model to describe the adsorption kinetics (Aboudzadeh *et al.*, 2006; Lua and Jia, 2009). Nevertheless, there are no established criteria to decide when to couple either an isotherm equilibrium model or a kinetic model to the adsorber model when experimental data is lacking to describe the kinetic behaviour of the adsorbent in a fixed-bed adsorber at an industrial scale.

The main aim of this work was to elucidate when an equilibrium isotherm model or an apparent kinetic model should be coupled to a fixed-bed adsorber model in order to describe reliable breakthrough curves. Rhodamine B (RhB) was used as a dye model molecule and a Mexican abundant low-cost natural zeolite was used as the adsorbent. Since this material has not been evaluated in any previous studies, it has been characterised by means of N₂ physisorption and X-ray powder diffraction techniques. In the same sense, an experimental study of the adsorption of RhB on the natural zeolite at laboratory scale was carried out. In particular, equilibrium and kinetic observations were obtained at several temperatures, inlet RhB concentrations and particle diameters. Langmuir and Freundlich isotherm models were used to fit experimental equilibrium data. The kinetic experimental data were described by means of pseudo first order and pseudo second order kinetic models. Finally, two pseudo-heterogeneous models that accounted for convection, dispersion and interfacial mass transport phenomena coupled to adsorption kinetic phenomena were examined to predict breakthrough curves from the fixed-bed adsorber. One of these models, named the Linear Driving Force Model (LDF-M), made use of the most appropriate isotherm equilibrium model. The other model, named the Apparent Kinetic Adsorber Model (AkA-M), made use of the most appropriate apparent kinetic model that accounted for both diffusional mass transport phenomena and the adsorption kinetics itself. These modelling approaches were intentionally evaluated since they are suitable to describe with certainty and without computation restraints the possible behaviour of a new adsorbent in a fixed-bed adsorber at industrial scale.

Table 1. Characteristics of the Rhodamine B.

Parameter	Value	Parameter	Value
Suggested name	Rhodamine B	Solubility in water	0.78
C.I. number	45170	Solubility in ethanol	1.47
C.I. name	Basic Violet 10	Molecular size (nm) ^a	1.44×1.09×0.64
Class	Rhodamine	Empirical formule	C ₂₈ H ₃₁ N ₂ O ₃ Cl
Ionization	Basic	Molecular weight	479.029
λ_{\max} (nm)	554	CAS number	81-88-9

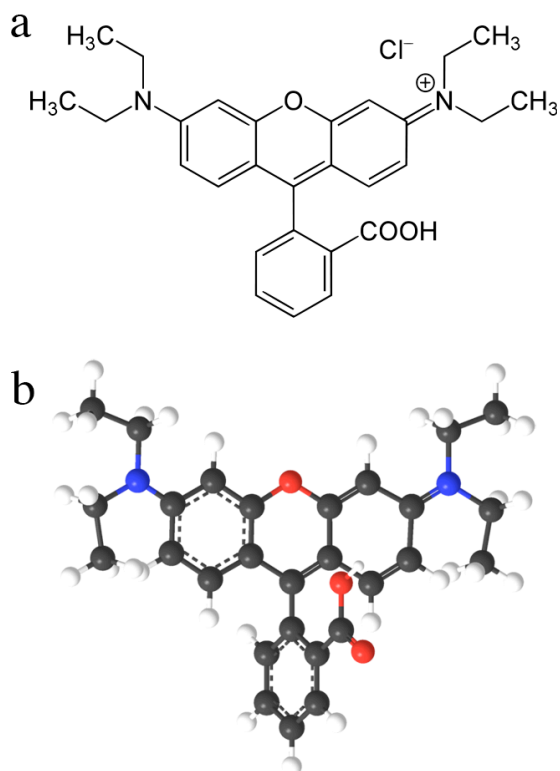
^aReference: Huang *et al.* (2008)

Fig. 1. Chemical structure of Rhodamine B. (a) cationic form (b) three-dimensional structure.

2 Procedures

2.1 Materials

A basic dye, RhB, purchased from the Sigma-Aldrich Chemical Company was used as a model molecule to evaluate the adsorption capacity of the natural zeolite. The properties of RhB are shown in Table 1 and its chemical structure is displayed in Fig. 1. A UV-Visible spectrophotometer (HACH DR 2800) at a wavelength of 554 nm was used to monitor RhB concentration through the use of the Beer-Lambert law.

The natural zeolite used in this study was obtained

from Etna municipality, Oaxaca, Mexico. This material was treated prior to the adsorption experiments. A sample of this material was crushed, sieved (16-20 mesh) and washed with deionised water in order to remove the dust attached to the surface. The washed sample was heated at 110 °C for 24 h to evaporate moisture from particles and to evaporate any volatile component that might have been adsorbed. The specific surface area of the natural zeolite was obtained from the physisorption of nitrogen using a Volumetric Quantachrome Autopore 1L-C instrument at -197 °C (at Mexico City 2250 m altitude). The specific surface area was calculated according to the standard Brunauer-Emmet-Teller (BET) method, and the average pore size was determined from the desorption branch of the isotherm using the Barrett-Joyner-Halenda (BJH) method (Barrett *et al.*, 1951). X-ray powder diffraction (XRD) was used to investigate the crystalline species and bulk phases present in the natural zeolite. XRD diffractograms presented in this study were obtained from a Siemens D-500 diffractometer employing a nickel-filtered Cu K α radiation ($\lambda = 1.5406 \text{ \AA}$, 40 kV, 30 mA) at 0.020° intervals in the range $20^\circ \leq 2\theta \leq 75^\circ$ with 1 s count accumulation per step directly from the natural zeolite.

2.2 Adsorption equilibrium

The adsorption equilibrium data were obtained by an immersion method at different RhB concentrations (10-200 mg/L) and temperatures (20, 35 and 50 °C). An isothermal well-stirred batch adsorber was fed with 0.25 g of the natural zeolite and 50 mL of RhB solution at the desired initial concentration. The adsorber was covered to avoid the evaporation of the RhB solution, and heated by a thermostat to the desired temperature. RhB concentration was monitored daily. The obtained data were used to calculate the RhB equilibrium concentrations. The amount of RhB adsorbed at equilibrium (q_{ne}) was calculated by a mass balance

equation given as follows:

$$q_{ne} = \frac{V(C_{no} - C_{ne})}{m} \quad (1)$$

where V is the volume of RhB solution fed to the adsorber, C_{no} is the initial concentration of RhB, C_{ne} is the RhB concentration in liquid phase at equilibrium, and m is the mass of the natural zeolite fed to the adsorber.

2.2.1. Isotherm model

The adsorption isotherm suggests how the RhB molecules distribute between the liquid phase and the solid phase when the adsorption process reaches equilibrium. The analysis of the observed equilibrium data by means of an appropriate isotherm model is used to characterise the adsorption capacity of a specific adsorbent and, from an engineering point of view, to design and optimise the adsorption process at an industrial scale when the isotherm model is coupled to the fixed-bed adsorber model. In this work Langmuir and Freundlich isotherm models were evaluated to fit our adsorption equilibrium observations with the aim to determine the best isotherm model to be coupled to the fixed-bed adsorber model to predict breakthrough curves, as presented further.

The Langmuir model assumes that adsorption occurs on a homogenous surface, where sites are equally available and energetically equivalent. Each site can adsorb at most one molecule of RhB and there are no interactions between RhB molecules on adjacent sites. (Al-Duri and Yong, 2000). The Langmuir model is given by:

$$q_{ne} = \frac{q_m K_L C_{ne}}{1 + K_L C_{ne}} \quad (2)$$

where q_{ne} is the amount of RhB adsorbed on a unit weight of adsorbent at equilibrium, C_{ne} is the concentration of RhB in liquid phase at equilibrium, q_m is the maximum amount of RhB adsorbed per unit weight of adsorbent at equilibrium, and K_L is the Langmuir adsorption constant related to RhB adsorption affinity on the adsorbent.

The Freundlich model accounts for Langmuir model weaknesses. This isotherm model assumes a heterogeneous surface, where each site can adsorb more than one molecule of RhB and there are interactions between RhB molecules on adjacent sites (Walker and Weatherley, 2001). The Freundlich

adsorption model is given by:

$$q_{ne} = K_F C_{ne}^{1/n} \quad (3)$$

where q_{ne} is the amount of RhB adsorbed on a unit weight of adsorbent at equilibrium, C_{ne} is the concentration of RhB in liquid phase at equilibrium, K_F and n are adsorption affinity constants.

2.2.2. Adsorption thermodynamics

Thermodynamic adsorption parameters were calculated from the dimensionless thermodynamic equilibrium constant, K_C , by means of the well-known modified Van't Hoff equation given by Equation (4) (Namasivayam and Ranganathan, 1995), that relates the change in temperature to the change in the equilibrium constant K_C , given the standard enthalpy change, ΔH° , and standard entropy change, ΔS° , for the adsorption process.

$$\ln K_C = \frac{\Delta S^\circ}{R} - \frac{\Delta H^\circ}{RT} \quad (4)$$

$$K_C = \frac{C_{ne}}{C_{nse}} \quad (5)$$

where C_{nse} and C_{ne} are the equilibrium concentrations of the RhB on adsorbent and in the solution respectively, R is the ideal gas constant and T is the system temperature. Standard Gibbs free energy, ΔG° (kJ/mol) at various temperatures was calculated through the following thermodynamic relation:

$$\Delta G^\circ = -RT \ln K_C \quad (6)$$

2.3 Adsorption kinetics

Kinetic experiments were carried out using a rotating basket batch adsorber operated isothermally (Carberry, 1976). The adsorber was heated by the use of a water bath to the desired temperature. A stainless steel propeller containing two rectangular baskets of 20 mm height, 16 mm width and 12 mm depth was used to stir this batch adsorber. Each basket was loaded with 2.5 g of adsorbent. For each experiment 500 mL of RhB solution at an initial desired concentration was added to the stirred batch adsorber. The effect of stirring speed (100-200 rpm), initial RhB concentration (10-200 mg/L), temperature (20, 35 and 50 °C) and particle size (1.0 and 2.5 mm) on adsorption rate was studied.

2.3.1. Kinetic model

Kinetics provides information regarding the mechanism and rate of adsorption of the adsorbate on a specific adsorbent. The development of a kinetic model is essential for designing and optimising an adsorption process. A pseudo-first-order kinetic model given by Equation (7) and a pseudo-second-order model given by Equation (8) are among the kinetic models most applied to adsorption processes (Ho and McKay, 1999a, b; Ho, 2006; Crini *et al.*, 2007; Wu *et al.*, 2009; Dawood and Sen, 2012; de la Peña-Torres *et al.*, 2012). In this work, these two kinetic models were evaluated to determine which one better describes our experimental kinetic observations, and hence to couple this kinetic model to the fixed-bed adsorber model to predict breakthrough curves, as presented in the following section. The kinetic models are given by:

$$\frac{dq_n}{dt} = k_1(q_{ne} - q_n) \quad (7)$$

$$\frac{dq_n}{dt} = k_2(q_{ne} - q_n)^2 \quad (8)$$

where q_{ne} is the amount of RhB adsorbed on a unit weight of adsorbent at equilibrium, q_n is the amount of RhB adsorbed on a unit weight of adsorbent, k_1 and k_2 are the adsorption rate constants and t is the adsorption time. Parameters involved in the isotherm and kinetic models were estimated by a multiresponse and multiparameter Levenberg-Marquardt method, considering a 95% confidence interval (Stewart *et al.*, 1992).

2.4 Fixed-bed adsorber model

With the aim of identifying some criteria for deciding when an equilibrium isotherm model or an apparent kinetic model should be coupled to the fixed-bed adsorber model to predict breakthrough curves for a determined adsorbent-adsorbate system, two pseudo heterogeneous models were evaluated to carry out a parametric sensitivity study of the fixed-bed adsorber. The first model, LDF-M, made use of an isothermal equilibrium model. The second model, AkA-M, made use of an apparent kinetic model. Both model approaches are totally accepted in literature to propose the preliminary dimension of an industrial fixed-bed adsorber elucidating the possible behaviour of a new and specific adsorbent, as in this study (Inglezakis and Grigoropoulou, 2004; Abu-Lail *et al.*, 2012).

These models were based on the following assumptions: (i) the kinetic model was apparent

since observations were obtained by using pellets of adsorbent where diffusional mass transport phenomena were involved; (ii) the fixed-bed adsorber was considered to be operated isothermally; (iii) the adsorbent pellets were assumed to be spheres of uniform size; (iv) there were no velocity profiles inside the fixed-bed adsorber since low values of inlet superficial velocity were accounted for and the tube to particle diameter ratio was greater than 12 (Castillo-Araiza and Lopez-Isunza, 2008); (v) the radial concentration gradients were considered to be insignificant; and (vi) the mass transport parameters (D_{ax} and k_L) were considered to be effective and were obtained from literature correlations (Wilson and Geankoplis, 1966; Chung and Wen, 1968).

The governing transport equations for the LDF-M are given by the following equations:

Fluid phase:

$$\varepsilon \frac{\partial C_n}{\partial t} + \rho_B \frac{\partial q_n}{\partial t} + v_z \varepsilon \frac{\partial C_n}{\partial z} = D_{ax} \varepsilon \frac{\partial^2 C_n}{\partial z^2} \quad (9)$$

Solid phase:

$$\rho_B \frac{\partial q_n}{\partial t} = (1 - \varepsilon) k_L a_v (C_n - C_{ns}^*) \quad (10)$$

The initial conditions are:

$$t = 0; \quad C_n = 0; q_n = 0, \quad \text{for } 0 < z < L \quad (11)$$

The boundary conditions are:

$$z = 0; \quad \varepsilon v_z C_n - \varepsilon D_{ax} \frac{\partial C_n}{\partial z} = v_z C_{no}; \quad \text{for } t > 0 \quad (12)$$

$$z = L; \quad \frac{\partial C_n}{\partial z} = 0; \quad \text{for } t > 0 \quad (13)$$

where D_{ax} is the axial dispersion coefficient, k_L is the so-called effective LDF mass transfer coefficient, a_v is the interfacial particle area per unit volume of the adsorbent pellet, C_n is the fluid phase concentration of the RhB, C_{ns}^* is the RhB liquid concentration at the liquid-solid interface, which is assumed to be at equilibrium with the prevailing solid phase concentration and hence its value was calculated by an isotherm model (Eqs. (3) or (4)), q_n is the amount of RhB adsorbed on a unit weight of adsorbent, v_z is the superficial axial velocity of the fluid, calculated as the ratio of the volumetric flow rate divided by the cross-sectional area of the bed, ε is the void fraction of the bed, ρ_B is the density of the bed, t is the operation time, and z is the axial position along the bed.

The governing transport equations for AkA-M are given by the following equations:

Fluid phase:

$$\varepsilon \frac{\partial C_n}{\partial t} + v_z \varepsilon \frac{\partial C_n}{\partial z} = D_{ax} \varepsilon \frac{\partial^2 C_n}{\partial z^2} - (1 - \varepsilon) k_L a_v (C_n - C_{ns}) \quad (14)$$

Solid phase:

$$(1 - \varepsilon) \frac{\partial C_{ns}}{\partial t} = (1 - \varepsilon) k_L a_v (C_n - C_{ns}) - \rho_B \frac{\partial q_n}{\partial t} \quad (15)$$

$$\frac{\partial q_n}{\partial t} = k_2 (q_{ne} - q_n)^n \quad (16)$$

The initial conditions are:

$$t = 0; \quad C_n = 0, C_{ns} = 0 \quad \text{and} \quad q_n = 0 \quad \text{for} \quad 0 < z < L \quad (17)$$

The boundary conditions are:

$$z = 0; \quad v_z C_n - D_{ax} \frac{\partial C_n}{\partial z} = v_z C_{no} \quad \text{for} \quad t > 0 \quad (18)$$

$$z = L; \quad \frac{\partial C_n}{\partial z} = 0 \quad \text{for} \quad t > 0 \quad (19)$$

The models solved in this section are given by sets of parabolic partial differential equations, which were solved numerically by the method of orthogonal collocation using 30 interior points of placement in axial coordinates, employing shifted Legendre polynomials for obtaining the collocation points (Finlayson, 1980). The reduced set of ordinary differential equations was integrated by the Runge-Kutta-Fehlberg method (Lapidus and Seinfeld, 1971).

2.4.1. Mass transfer correlations

The axial dispersion coefficient was calculated from the equation suggested by Chung and Wen (1968).

$$Pe = \frac{0.2 + 0.011 Re_p^{0.48}}{\varepsilon} \quad (20)$$

$$Pe = \frac{d_p v_z}{D_{ax}} \quad (21)$$

$$Re_p = \frac{d_p v_z}{\nu} \quad (22)$$

where Pe is the Péclet number, Re_p is the particle Reynolds number, d_p is the particle diameter, ν is the kinematic viscosity of the solution, and ε is the void fraction of the bed, which for this study was obtained from the empirical equation proposed by de Klerk (2003). The interfacial mass transfer coefficient was calculated according to the correlation of Wilson and Geankoplis (1966).

$$Sh = \frac{1.09}{\varepsilon} Re_p^{0.33} Sc^{0.33} \quad (23)$$

$$Sc = \frac{\nu}{D_{RhB}} \quad (24)$$

$$Sh = \frac{k_L \cdot d_p}{D_{RhB}} \quad (25)$$

where Sh is the Sherwood number, Sc is the Schmidt number and D_{RhB} is the diffusion coefficient of RhB in water and was calculated by the equation developed by Wilke and Chang (1955).

3 Results and discussion

3.1 Natural zeolite characterisation

An X-ray diffraction pattern for the utilised natural zeolite is shown in Fig. 2. It consisted of a clay-quartz material with crystalline structure, predominantly containing clinoptilolite and to a lesser extent mordenite. The isotherm obtained by nitrogen physisorption is presented in Fig. 3. The adsorption-desorption isotherm observed was of type IV. Capillary condensation and the capillary evaporation occurred at almost the same relative pressures but did not change the shape of the hysteresis loop, indicating that a kinetic equilibrium of capillary condensation-evaporation existed in the mesopores. The hysteresis loop at higher-relative pressures was a consequence of N₂ filling the textural pores that were associated with the natural zeolite morphology (Gomonaj *et al.*, 2000). Surface area, average pore volume and pore diameter of the natural zeolite are given in Table 2. The surface area was similar to that obtained for other natural zeolites of the same type (10-20 m²/g) used to remove contaminants from effluents (Motsi *et al.*, 2009; Camacho *et al.*, 2011). Pore volume and pore diameter of the natural zeolite were larger than RhB dimensions (see Table 1), suggesting that RhB might access the pores of the adsorbent without space restrictions.

Table 2. Physical characteristics of the natural zeolite

Properties	Values
Surface area (m ² /g)	14
Average pore diameter (nm)	15
Pore volume (cc/g)	0.054

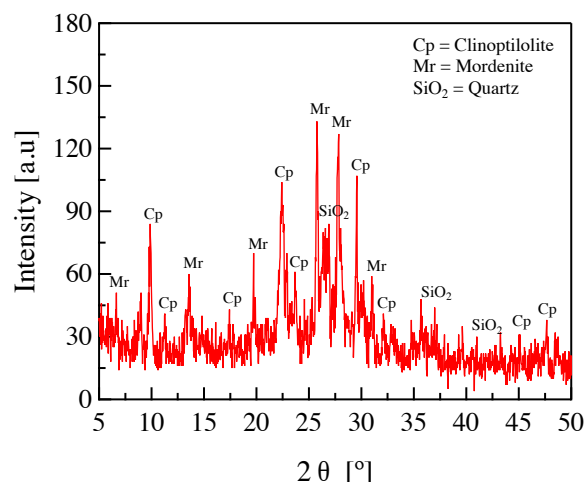


Fig. 2. X-ray diffraction patterns of the natural zeolite.

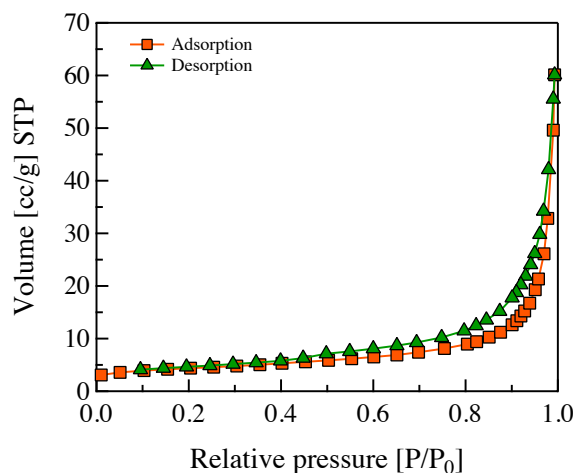


Fig. 3. Nitrogen adsorption/desorption isotherm of the natural zeolite.

3.2 Adsorption isotherm of RhB

A comparison between the observed and fitted adsorption capacity of the natural zeolite (q_{ne}) as a function of time at different temperatures is presented in Fig 4. Adsorption equilibrium observations were fitted by means of Langmuir and Freundlich isotherm models. A non-linear relationship between the amount of RhB adsorbed and RhB concentration in the solution at equilibrium was observed. The adsorption capacity of the natural zeolite decreased as the temperature increased, as a result of the exothermicity of the adsorption process. Vimonses *et al.* (2009) reported similar results for Congo Red adsorption on clays, concluding that the lower adsorption capacities of the adsorbent at higher temperatures was due to a

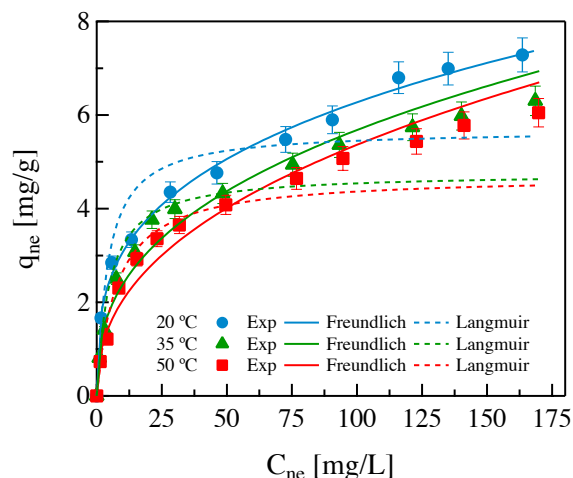


Fig. 4. Adsorption isotherms of Rhodamine B onto natural zeolite at various temperatures.

weaker bonding between the hydrogen from the dye and adsorbent, and to a weaker Van der Waals type interaction between the dye and adsorbent caused by an apparent increment in the vibrational energy of adsorbed dye leading to its desorption.

The estimated equilibrium parameters involved in the Langmuir and Freundlich isotherm models are presented in Table 3. The regression and parameters were statistically significant. The parameters were not statistically correlated since components in the variance-covariance matrix were lower than (\pm) 0.95. Nevertheless, the R^2 for the Freundlich isotherm model was greater than the R^2 for the Langmuir isotherm model. The Freundlich model led to better predictions than the Langmuir model at initial RhB concentrations higher than 60 mg/L. Therefore, the Freundlich isotherm model was preferred over the Langmuir model to account for kinetics in the LDF-M to predict breakthrough curves from the adsorption fixed-bed column. Estimated thermodynamic parameters at different temperatures were calculated using Eqs. (4)-(6). The average estimated value of ΔG° 16.8 kJ/mol at the studied temperatures indicated a spontaneous physical adsorption of RhB onto the natural zeolite (Krishna and Bhattacharyya, 2002; Chu *et al.*, 2004). This spontaneous process was consequence of the exothermicity of the adsorption process ($\Delta H^\circ = -15.7$ kJ/mol) and to a favourable adsorption disorder of RhB on the natural zeolite ($\Delta S^\circ = 3.7$ J/mol K).

Table 3. Langmuir and Freundlich parameters for Rhodamine B adsorption onto natural zeolite.

Temperature (°C)	Langmuir			Freundlich		
	q_m	K_L	R^2	K_F	n	R^2
20	5.6818	0.2351	0.9203	1.5046	3.2254	0.9899
35	4.7594	0.2072	0.9594	1.0020	2.6544	0.9656
50	4.6981	0.1308	0.9564	0.7803	2.3889	0.9604

Table 4. Kinetic parameters calculated for adsorption of Rhodamine B onto Natural Zeolite.

Parameters					Kinetic models					
T (°C)	C_{no} (mg/L)	d_p (mm)	Stirring speed (rpm)	$q_{ne}(exp)$ (mg/g)	Pseudo first order model			Pseudo second order model		
					$q_{ne}(cal)$	k_1	R^2	$q_{ne}(cal)$	k_2	R^2
20	10	1.0	200	1.2148	0.9813	0.0341	0.8802	1.2253	0.1048	0.9752
20	20	1.0	200	2.3430	1.5026	0.0523	0.9705	2.4032	0.1146	0.9973
20	50	1.0	200	3.4515	1.8635	0.0462	0.9723	3.4990	0.1009	0.9978
20	100	1.0	200	4.8047	2.4188	0.0459	0.9612	4.8581	0.0823	0.9983
35	20	1.0	200	2.1025	1.1755	0.0455	0.9457	2.1437	0.1479	0.9984
50	20	1.0	200	1.9714	1.0916	0.0520	0.9044	2.0208	0.1613	0.9988
20	20	2.5	200	1.5042	1.2879	0.0522	0.9830	1.6005	0.0815	0.9955

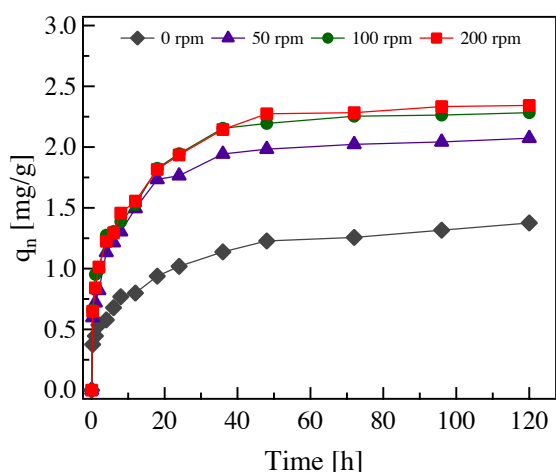


Fig. 5. Effect of the stirring speed for the adsorption of Rhodamine B on natural zeolite.

3.3 Kinetics of RhB adsorption

The influence of the stirring speed on the adsorption capacity of the natural zeolite as a function of time is presented in Fig. 5. These observations suggested that 200 rpm is a suitable stirring speed to carry out kinetic experiments in the absence of interparticle mass transport resistances, because there is no significant difference in the adsorption capacity of the natural zeolite at stirring speeds over 100 rpm. A comparison

between kinetic experiments and their fitting by the pseudo second order model is presented in Fig. 6. The effect of the initial RhB concentration on the adsorption capacity of the natural zeolite over time at an adsorption temperature of 20 °C, with an adsorbent mass of 2.5 g and adsorbent particles of 1 mm, is displayed in Fig. 6a. The adsorption of RhB on the natural zeolite took place during the first 50 h, suggesting that the interaction between kinetics and intraparticle mass transport phenomena played an important role on the RhB adsorption dynamics. The adsorption capacity of the natural zeolite increased as the initial concentration of RhB was increased, as is also observed in equilibrium experiments. So far at higher initial RhB concentrations an increase in the RhB concentration gradient (driving force) between the RhB in the solution and the RhB into the adsorbent favoured the adsorption capacity of the natural zeolite (Jain and Shrivastava, 2008). The effect of temperature on the adsorption capacity of the natural zeolite as a function of time at an initial RhB concentration of 20 mg/L, with an adsorbent mass of 2.5 g and adsorbent particles of 1 mm, is presented in Fig. 6b. Because of the exothermic nature of the adsorption process, a slight decrease in the adsorption capacity of the natural zeolite was observed when the adsorption temperature was increased.

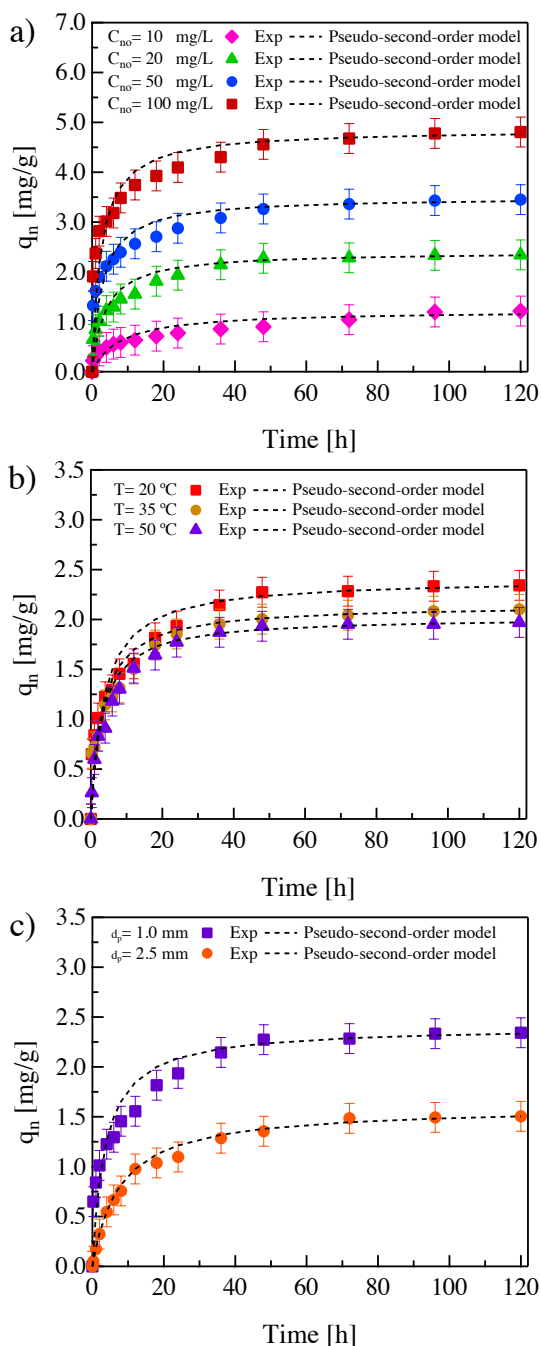


Fig. 6. Kinetic adsorption of Rhodamine B onto natural zeolite for various: (a) initial dye concentration (b) temperatures and (c) particles sizes.

Finally, the influence of the adsorbent particle size on the adsorption capacity as a function of time at an initial RhB concentration of 20 mg/L, with an adsorbent mass of 2.5 g and an adsorption temperature of 20 °C, is presented in Fig. 6c. Even

though diffusional mass transport resistances in the natural zeolite were apparently significant for both pellet sizes, a decrease in the pellet size led to an increase in the adsorbent interfacial area, being the main aspect favouring the adsorption capacity of the natural zeolite.

Apparent kinetic parameters estimated from the pseudo first order and pseudo second order models are presented in Table 4. Despite the fact that the kinetic parameters accounted for intraparticle diffusion mass transport resistances, these parameters and the regression were statistically significant. The parameters were not statistically correlated. Nevertheless, the R^2 indicated that the pseudo second order kinetic model better fitted kinetic data than the pseudo first order kinetic model. Therefore the pseudo second order kinetic model was used to account for adsorption kinetics and intraparticle mass transport diffusion into the AkA-M to predict breakthrough curves from the adsorption fixed-bed column.

3.4 Fixed-bed adsorber modelling

In this section LDF-M and AkA-M were evaluated to predict breakthrough curves from an industrial-scale adsorption column packed with a natural zeolite during the removal of RhB under the conditions presented in Table 5. In particular, breakthrough curves were predicted at inlet RhB concentrations varying from 10 to 100 mg/L (see Fig. 7), at inlet superficial velocities varying from 1.8 to 9.0 m/h (see Fig. 8), at column temperatures varying from 20 °C to 50 °C (see Fig. 9), at column lengths varying from 1 to 2.5 m (see Fig. 10), and at particle diameters varying from 1.0 to 5.0 mm (see Fig. 11).

Predictions of breakthrough curves at different initial RhB concentrations were obtained considering a 1.5 m column length packed with adsorbent particles of 1 mm, operated at a superficial velocity of 3.6 m/h and a constant temperature of 20 °C. Saturation time was affected by inlet RhB concentration, as observed in Fig. 7. Even though both models predicted an earlier saturation time as the inlet RhB concentration was increased, LDF-M led to steeper slopes of the breakthrough curves than AkA-M. The breakthrough slopes projected by the LDF-M indicated a negligible effect of dispersion, inter or intraparticle mass transport resistances on the adsorption process and, hence, saturation time was essentially a function of the amount of available adsorption active sites. Since LDF-M simulations indicated that dispersion, and interparticle mass transport resistances were

Table 5 Operational conditions used in bed column simulations

Simulation	C_{no} (mg/L)	d_p (cm)	v_z (m/h)	ε	T (°C)	L_t (cm)	d_c (cm)
1	20	0.10	1.8	0.383	20	150	10
2	20	0.10	2.7	0.383	20	150	10
3	20	0.10	3.6	0.383	20	150	10
4	20	0.10	9.0	0.383	20	150	10
5	10	0.10	3.6	0.383	20	150	10
6	50	0.10	3.6	0.383	20	150	10
7	100	0.10	3.6	0.383	20	150	10
8	20	0.10	3.6	0.383	20	100	10
9	20	0.10	3.6	0.383	20	200	10
10	20	0.10	3.6	0.383	20	250	10
11	20	0.10	3.6	0.383	35	150	10
12	20	0.10	3.6	0.383	50	150	10
13	20	0.25	3.6	0.383	20	150	10
14	20	0.50	3.6	0.383	20	150	10

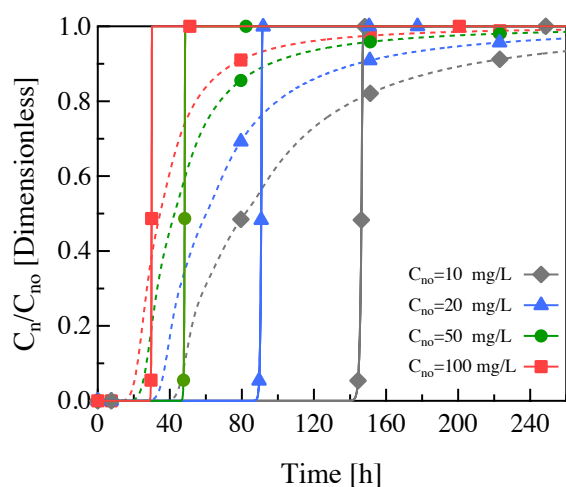


Fig. 7. Effect of the inlet concentration on the theoretical breakthrough curves. The model using the LDF-M (—); and the model that uses the AkA-M model (- - -). (T=20 °C, d_p =1 mm, v_z =3.6 m/h, L_t =150 cm).

insignificant, AkA-M predicted breakthrough curves whose slope essentially indicated the presence of intraparticle mass transport resistances. These intraparticle mass transport resistances were more significant at a lower inlet RhB concentration because of the role of the concentration gradient (driving force) on the diffusion-adsorption process discussed in Section 3.3. These simulations suggested that the AkA-M was more suitable than LDF-M to predict breakthrough curves, since intraparticle mass transport resistances were accounted for by the apparent kinetic model rather than by the isotherm model used to account for adsorbate-adsorbent interactions.

Predictions for the breakthrough curves at different initial superficial velocities were obtained by considering a 1.5 m column length packed with adsorbent particles of 1 mm and operated at an inlet RhB concentration of 20 mg/L and a constant temperature of 20 °C. Breakthrough curves were sensitive to inlet superficial velocity, as shown in Fig. 8. Both LDF-M and AkA-M models predicted breakthrough curves that were affected by the residence time of RhB in the fixed-bed column, i.e. the saturation time was larger at lower inlet superficial velocities since a higher residence time favoured RhB transport from the bulk to the active sites on the natural zeolite (Han *et al.*, 2009). Nevertheless, LDF-M predicted steeper breakthrough slopes than AkA-M, corroborating that LDF-M was not able to account for intraparticle mass transport phenomena involved in a natural zeolite presenting diffusion limitations such as the one studied in this work.

Predictions of the breakthrough curves varying column temperature from 20 to 50 °C were obtained at an inlet RhB concentration of 20 mg/L, an inlet superficial velocity of 3.6 m/h, and a column of 1.5 m length packed with adsorbent particles of 1 mm. The breakthrough curve was slightly affected by temperature, as shown in Fig. 9. As in the previous results, both models, LDF-M and AkA-M, predicted different breakthrough curves but similar adsorption tendencies as reported by Bhuvaneshwari and Sivasubramanian (2014), i.e. a lower saturation time was obtained by decreasing the column temperature as a result of the exothermicity characteristics of the adsorption process discussed in Section 3.2.

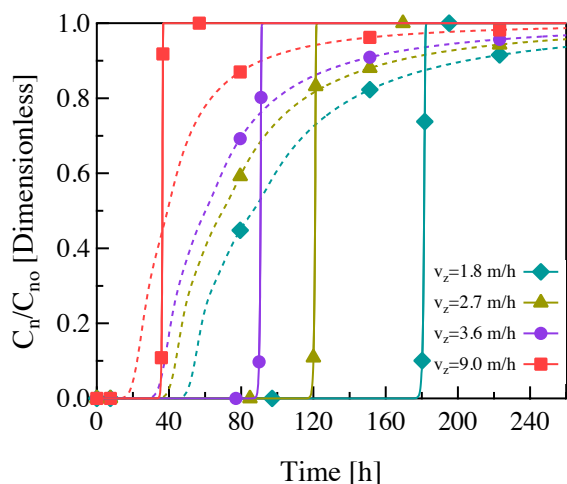


Fig. 8. Effect of the inlet superficial velocity on the theoretical breakthrough curves. The model using the LDF-M (—); and the model that uses the AKA-M model (- -). ($T=20\text{ }^{\circ}\text{C}$, $d_p=1\text{ mm}$, $C_{no}=20\text{ mg/L}$, $L_t=150\text{ cm}$).

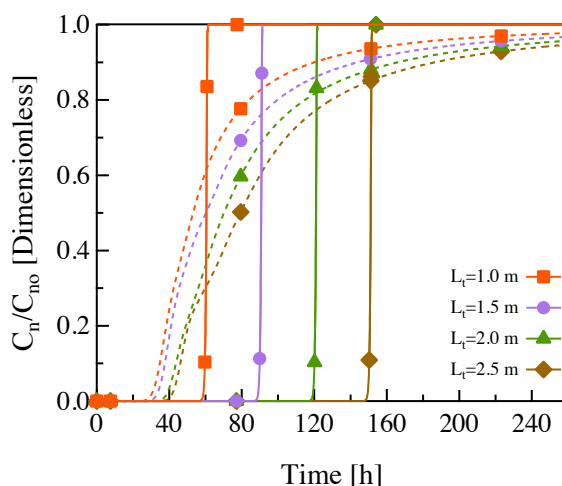


Fig. 10. Effect of the bed length on theoretical breakthrough curves. The model using the LDF-M (—); and the model that uses the AKA-M model (- -). ($T=20\text{ }^{\circ}\text{C}$, $d_p=1\text{ mm}$, $v_z=3.6\text{ m/h}$, $C_{no}=20\text{ mg/L}$).

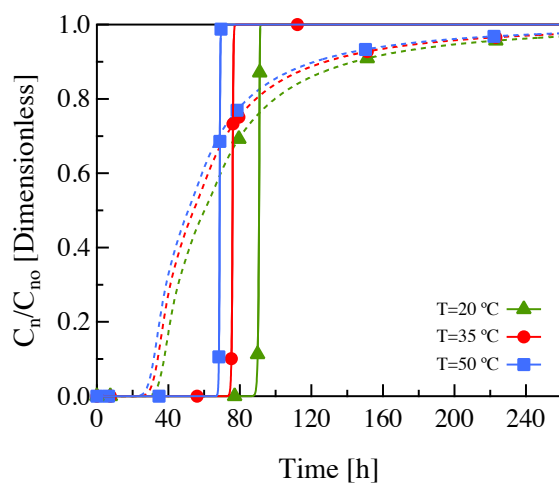


Fig. 9. Effect of the temperature on theoretical breakthrough curves. The model using the LDF-M (—); and the model that uses the AKA-M model (- -). ($C_{no}=20\text{ mg/L}$, $d_p=1\text{ mm}$, $v_z=3.6\text{ m/h}$, $L_t=150\text{ cm}$).

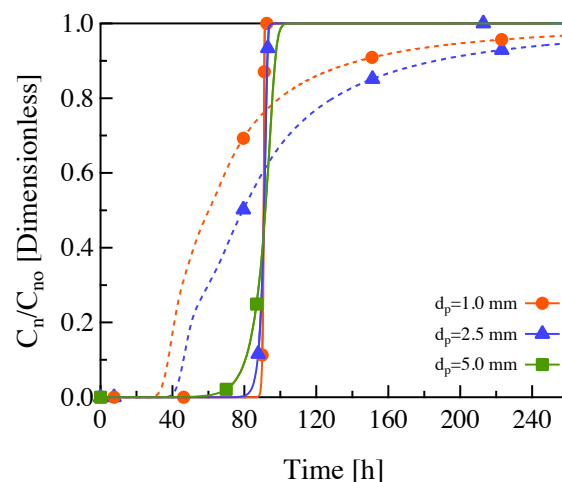


Fig. 11. Effect of the particle size on theoretical breakthrough curves. The model using the LDF-M (—); and the model that uses the AKA-M model (- -). ($T=20\text{ }^{\circ}\text{C}$, $C_{no}=20\text{ mg/L}$, $v_z=3.6\text{ m/h}$, $L_t=150\text{ cm}$).

Predictions of the breakthrough curves when varying the column length from 1 to 2.5 m were obtained by considering adsorbent particles of 1 mm, an inlet superficial velocity of 3.6 m/h, an inlet RhB concentration of 20 mg/L and a constant temperature of 20 °C. Since the residence time of RhB and the amount of adsorbent was a function of the column length, LDF-M and AKA-M predictions indicated that the saturation capacity of the fixed-bed column was favoured at larger column lengths, as shown in Fig. 10

and observed from other adsorption studies (Xu *et al.*, 2013).

Predictions of breakthrough curves when varying the particle diameter of adsorbent packed in the column from 1.0 to 5.0 mm were obtained at an inlet RhB concentration of 20 mg/L an inlet superficial velocity of 3.6 m/h, a constant temperature of 20 °C and with a column length of 1.5 m. LDF-M accounted for the role of particle size on interparticle mass transport phenomena, predicting an increase in the saturation time and a slight change

in the steepness of the breakthrough slope as the particle size decreased (see Fig. 11). Smaller particle sizes favoured the interfacial mass transfer of RhB from the bulk to the adsorbent increasing column saturation capacity. Based on these simulations, AkA-M predicted breakthrough curves whose slopes indicated the presence of both inter and intraparticle mass transport phenomena, but mainly intraparticle as aforementioned and observed from other adsorption studies when adsorbents are evaluated at industrial scale (Marin *et al.*, 2014).

Conclusions

Certain general points might be deduced from the experimental and simulation analysis on the prediction of Rhodamine B adsorption on a Mexican natural zeolite:

1. The zeolite used as adsorbent was adequate for RhB separation from aqueous solution. Increasing contact time, zeolite amount and dye concentrations resulted in increased adsorption, while the reverse effect was observed by increasing the temperature and zeolite particle size.
2. Based on statistical analysis it was found that the best fit of the equilibrium adsorption data was obtained with the Freundlich model, and that the kinetic behaviour was described by a pseudo-second order model. Thermodynamic results indicated that the adsorption of RhB is spontaneous and exothermic.
3. The two models, LDF-M and AkA-M, considered for describing fixed-bed adsorption of RhB on the natural zeolite showed similar tendencies regarding the effect on the breakthrough point of the different parameters considered. However the shapes of the breakthrough curves predicted by both models were significantly different. For all the conditions considered in the simulations, the slopes for LDF-M breakthrough curves were much steeper than those predicted by AkA-M. Furthermore, the breakthrough point times were always found to be larger for the LDF-M under similar conditions, to the extent of being up to three times larger than those predicted by AkA-M. Such differences between the breakthrough point times were reduced by modifying the

operating conditions that favoured particle surface saturation, such as increasing the inlet RhB concentration and the superficial liquid velocity as well as by reducing the bed height.

From these results AkA-M is a simple but necessary first approach to model the industrial behaviour of porous adsorbents when the resistances to mass transport by diffusion of adsorbate are significant. Nevertheless, experimental and modelling studies accounting for explicitly the diffusion phenomena of the natural zeolite have to be carried out further.

Acknowledgments

The first author (G. Che-Galicia) is grateful for the graduate scholarship provided by the Consejo Nacional de Ciencia y Tecnología (CONACyT). The authors also acknowledge to Dr. Miguel A. Hernández Espinosa for providing the natural zeolite.

Nomenclature

Roman letters

a_v	mass transfer area per unit volume of the particle, m^{-1}
C_n	concentration of Rhodamine B in fluid phase, mg/L
C_{ne}	concentration of Rhodamine B at equilibrium in fluid phase, mg/L
C_{no}	initial concentration of Rhodamine B in fluid phase, mg/L
C_{ns}	concentration of Rhodamine B in the adsorbent surface, mg/L
C_{nse}	concentration of Rhodamine B at equilibrium in the adsorbent, mg/L
d_c	column diameter, cm
d_p	particle diameter, m
D_{ax}	axial dispersion coefficient, m^2/h
D_{RHB}	molecular diffusion coefficient of Rhodamine B in water, m^2/s
k_1	kinetic constant for the pseudo first order reaction, h^{-1}
k_2	kinetic constant for the pseudo second order reaction, $g/(mg\ h)$
k_L	external mass transfer coefficient in fluid phase, m/h
K_c	adsorption equilibrium constant
K_F	Freundlich isotherm constant, $(mg^{1-1/n}\ L^{1/n})/g$
K_L	Langmuir isotherm constant, L/mg
L_t	length of the column, cm
m	mass of natural zeolite, g

n	Freundlich isotherm constant
q_m	Langmuir isotherm constant, mg/g
q_n	mass of Rhodamine B adsorbed per unit mass of natural zeolite, mg/g
q_{ne}	mass of Rhodamine B adsorbed at equilibrium, mg/g
R	ideal gas constant, 8.314 J/(mol K)
t	time, h
T	temperature, K
v_z	interstitial fluid velocity in the z direction, m/h
V	volume of the Rhodamine B solution, L
z	distance in the axial direction of the column, m
<i>Greek letters</i>	
ε	void fraction of the bed
ρ_B	bed density, kg/m ³
ν	kinematic viscosity, m ² /h
ΔG^o	Gibbs free energy, kJ/mol
ΔH^o	enthalpy, kJ/mol
ΔS^o	entropy, J/(mol K)

References

- Abouzadeh, M.R., Jiawen, Z., Bin, W. (2006). Simulation of protein adsorption in a batchwise affinity chromatography with a modified rate model. *Korean Journal of Chemical Engineering* 23, 997-1002.
- Abu-Lail, L., Bergendahl, J. A., Thompson, R. W. (2012), Mathematical modeling of chloroform adsorption onto fixed-bed columns of highly siliceous granular zeolites. *Environmental Progress & Sustainable Energy* 31, 591-596.
- Al-Duri, B., Yong, Y.P. (2000). Lipase immobilisation: an equilibrium study of lipases immobilised on hydrophobic and hydrophilic/hydrophobic supports. *Biochemical Engineering Journal* 4, 207-215.
- Barrett, E.P., Joyner, L.G., Halenda, P.P. (1951) The determination of pore volumen and area distributions in porous substances. i. computations from nitrogen isotherms. *Journal American Chemistry Society* 73, 373-380.
- Bhuvaneshwari, S., Sivasubramanian, V. (2014). Equilibrium, kinetics, and breakthrough studies for adsorption of Cr(vi) on chitosan. *Chemical Engineering Communications* 201, 834-854.
- Marin, P., Borba, C.E., Módenes, A.N., Espinoza-Quiñones, F.R., de Oliveira, S.P.D., Kroumov, A.D. (2014). Determination of the mass transfer-limiting step of dye adsorption onto commercial adsorbent by using mathematical models. *Environmental Technology* 35, 2356-2364.
- Camacho, L.M., Parra, R.R., Deng, S. (2011). Arsenic removal from groundwater by MnO₂-modified natural clinoptilolite zeolite: effects of pH and initial feed concentration. *Journal of Hazardous Materials* 189, 286-293.
- Carberry, J.J. (1976). *Chemical and Catalytic Reaction Engineering*. McGraw-Hill, New York.
- Castillo-Araiza, C.O., Lopez-Isunza, F. (2008). Hydrodynamic models for packed beds with low tube-to-particle diameter ratio. *International Journal of Chemical Reactor Engineering* 6 (A1), 1-14.
- Chern, J.M., Chien, Y.M. (2001). Adsorption isotherms of benzoic acid onto activated carbon and breakthrough curves in fixed-bed columns. *Industrial & Engineering Chemistry Research* 40, 3775-3780.
- Chu, B.S., Baharin, B.S., Man, Y.B.C., Quek, S.Y. (2004). Separation of vitamin E from palm fatty acid distillate using silica: I Equilibrium of batch adsorption. *Journal of Food Engineering* 62, 97-103.
- Chung, S.F., Wen, C.Y. (1968). Longitudinal dispersion of liquid flowing through fixed and fluidized beds. *AIChE Journal* 14, 857-866.
- Crini, G. (2006). Non-conventional low-cost adsorbents for dye removal: a review. *Bioresource Technology* 97, 1061-1085.
- Crini, G., Peindy, H.N., Gimbert, F., Robert, C. (2007). Removal of C.I. Basic Green 4 (Malachite Green) from aqueous solutions by adsorption using cyclodextrin-based adsorbent: kinetic and equilibrium studies. *Separation and Purification Technology* 53, 97-110.
- Crittenden, J.C., Weber, W.J. (1978). Predictive model for design of fixed-bed adsorbers: parameter estimation and development. *Journal of the Environmental Engineering Division* 104, 185-197.

- de Klerk, A. (2003). Voidage variation in packed beds at small column to particle diameter ratios. *Journal of American Institute of Chemical Engineers* 49, 2022-2029.
- De la Peña-Torres, A., Cano-Rodríguez, I., Aguilera-Alvarado, A.F., Gamiño-Arroyo, Z., Gómez-Castro, F.I. Gutiérrez-Valtierra, M.P., Soriano-Pérez S. (2012). Arsenic adsorption and desorption on synthetic iron oxyhydroxides as study model to explain one of the mechanisms for its lixiviation from mining tailings. *Revista Mexicana de Ingeniería Química* 11, 495-503.
- Dawood, S., Sen, T.K. (2012). Removal of anionic dye Congo Red from aqueous solution by raw pine and acid-treated pine cone powder as adsorbent: equilibrium, thermodynamic, kinetics, mechanism and process design. *Water Research* 46, 1933-1946.
- Finlayson, B.A. (1980). *Nonlinear Analysis in Chemical Engineering*. McGraw-Hill, New York.
- Gomonaj, V., Gomonaj, P., Golub, N., Szekeresh, K., Charmas, B., Lebeda, R. (2000). Compatible adsorption of strontium and zinc ions as well vitamins on zeolites. *Adsorption Science and Technology* 18, 295-306.
- Hall, K.R., Eagleton, L.C., Acrivos, A., Vermeulen, T. (1966). Pore- and solid-diffusion kinetics in fixed-bed adsorption under constant-pattern conditions. *Industrial and Engineering Chemistry Fundamentals* 5, 212-223.
- Han, R., Wang, Y., Zhao, X., Wang, Y., Xie, F., Cheng, J., Tang, M. (2009). Adsorption of methylene blue by phoenix tree leaf powder in a fixed-bed column: Experiments and prediction of breakthrough curves. *Desalination* 245, 284-297
- Ho, Y.S. (2006). Review of second-order models for adsorption systems. *Journal of Hazardous Materials* 136, 681-689.
- Ho, Y.S., McKay, G. (1999a). The sorption of lead (II) ions on peat. *Water Research* 33, 578-584.
- Ho, Y.S., McKay, G. (1999b). Pseudo-second order model for sorption processes. *Process Biochemistry* 34, 451-465.
- Huang, J.H., Huang, K.L., Liu, S.Q., Wang, A.T., Yan, C. (2008). Adsorption of Rhodamine B and methyl orange on a hypercrosslinked polymeric adsorbent in aqueous solution. *Colloids and Surfaces A: Physicochemical and Engineering Aspects* 330, 55-61.
- Hutzler, N.J., Crittenden, J.C., Gierke, J.S., Johnson, A.S. (1986). Transport of organic compounds with saturated groundwater flow: experimental results. *Water Resources Research* 22, 285-295.
- Inglezakis, V.J., Grigoropoulou, H. (2004). Effects of operating conditions on the removal of heavy metals by zeolite in fixed bed reactors. *Journal of Hazardous Materials* 112, 37-43.
- Jain, R., Shrivastava, M. (2008). Adsorptive studies of hazardous dye Tropaeoline 000 from an aqueous phase on to coconut-husk. *Journal of Hazardous Materials* 158, 549-556.
- Ko, D.C.K., Porter, J.F., McKay, G. (2001). Film-pore diffusion model for the fixed-bed sorption of copper and cadmium ions onto bone char. *Water Research* 35, 3876-3886.
- Krishna, D.G., Bhattacharyya, G. (2002). Adsorption of methylene blue on kaolinite. *Applied Clay Science* 20, 295-300.
- Lapidus, L., Seinfeld, J.H. (1971). *Numerical Solution of Ordinary Differential Equations*. Academic Press, New York.
- Liao, H.T., Shiau, C.Y. (2000). Analytical solution to an axial dispersion model for the fixed-bed adsorber. *AIChE Journal* 46, 1168-1176.
- Lua, A.C., Jia, Q. (2009). Adsorption of phenol by oil-palm-shell activated carbons in a fixed bed. *Chemical Engineering Journal* 150, 455-461.
- Marshall, W.R., Pigford, R.L. (1947). *Application of Differential Equations to Chemical Engineering Problems*. University of Delaware Press, Newark.
- Motsi, T., Rowson, N.A., Simmons, M.J.H. (2009). Adsorption of heavy metals from acid mine drainage by natural zeolite. *International Journal of Mineral Processing* 92, 42-48.
- Namasivayam, C., Kavitha, D. (2002). Removal of Congo Red from water by adsorption onto activated carbon prepared from coir pith, an

- agricultural solid waste. *Dyes and Pigments* 54, 47-58.
- Namasivayam, C., Ranganathan, K. (1995). Removal of Cd (II) from wastewater by adsorption on "waste" Fe(III)/Cr(III) hydroxide. *Water Research* 29, 1737-1744.
- Osma, J.F., Saravia, V., Toca-Herrera, J.L., Couto, S.R. (2007). Sunflower seed shells: a novel and effective low-cost adsorbent for the removal of the diazo dye Reactive Black 5 from aqueous solutions. *Journal of Hazardous Materials* 147, 900-905.
- Özcan, A.S., Erdem, B., Özcan, A. (2005). Adsorption of Acid Blue 193 from aqueous solutions onto BTMA-bentonite. *Colloids and Surfaces A: Physicochemical and Engineering Aspects* 266, 73-81.
- Rafatullah, M., Sulaiman, O., Hashim, R., Ahmad, A. (2010). Adsorption of methylene blue on low-cost adsorbents: a review. *Journal of Hazardous Materials* 177, 70-80.
- Robinson, T., McMullan, G., Marchant, R., Nigam, P. (2001). Remediation of dyes in textile effluent: a critical review on current treatment technologies with a proposed alternative. *Bioresource Technology* 77, 247-255.
- Romero-González, J., Cano-Rodríguez, I., Walton, J.C., Peralta-Videa, J. R., Rodríguez E., Gardea-Torresdey J. L. (2005). A model to describe the adsorption and reduction of Cr (vi) from an aqueous solution by agave lechuguilla biomass. *Revista Mexicana de Ingeniería Química* 4, 261-272.
- Ruthven, D.M. (1984). *Principles of Adsorption and Adsorption Processes*. John Wiley and Sons, New York.
- Sankararao, B., Gupta, S.K. (2007). Modeling and simulation of fixed bed adsorbers (FBAs) for multi-component gaseous separations. *Computers and Chemical Engineering* 31, 1282-1295.
- Stewart, W.E., Caracotsios, M., Sørensen, J.P. (1992). Parameter estimation from multiresponse data. *AIChE Journal* 38, 641-650.
- Tien, C. (1994). *Adsorption Calculation and Modeling*. Butterworth-Heinemann, Boston.
- Vimonses, V., Lei, S., Jin, B., Chow, C.W.K., Saint, C. (2009). Kinetic study and equilibrium isotherm analysis of Congo Red adsorption by clay materials. *Chemical Engineering Journal* 148, 354-364.
- Walker, G., Weatherley, L. (2001). Adsorption of dyes from aqueous solution-the effect of adsorbent pore size distribution and dye aggregation. *Chemical Engineering Journal* 83, 201-206.
- Wang, S., Peng, Y. (2010). Natural zeolites as effective adsorbents in water and wastewater treatment. *Chemical Engineering Journal* 156, 11-24.
- Weber, W. J. (1972). *Physicochemical Processes for Water Quality Control*. John Wiley and Sons, New York.
- Wilke, C.R., Chang, P. (1955). Correlation of diffusion coefficients in dilute solutions. *AIChE Journal* 1, 264-270.
- Wilson, E.J., Geankoplis, C.J. (1966). Liquid mass transfer at very low Reynolds numbers in packed beds. *Industrial and Engineering Chemistry Fundamentals* 5, 9-14.
- Wu, F.C., Tseng, R.L., Huang, S.C., Juang, R.S. (2009). Characteristics of pseudo-second-order kinetic model for liquid-phase adsorption: a mini-review. *Chemical Engineering Journal* 151, 1-9.
- Xu, X., Gao, B., Tan, X., Zhang, X., Yue, Q., Wang, Y., Li, Q. (2013). Nitrate adsorption by stratified wheat straw resin in lab-scale columns. *Chemical Engineering Journal* 226, 1-6.